Progress In Electromagnetics Research C, Vol. 74, 9–17, 2017

A Novel Z-EBG Structure Embedded by DBCSRR for Suppression of Simultaneous Switching Noise

Xiu-Jie Hu[1, 2, *] and Zhi-Min Sun[1, 2]

Abstract—Aimed at solving the problems of high initial cutoff frequency, small stopband range and poor inhibition in the current electromagnetic band gap (EBG) structure, an electromagnetic band gap structure designed on the basis of periodic Z-bridge EBG inserted by a double complementary slit ring resonator (DBCSRR) cell is proposed. Compared with the traditional EBG structure, the proposed EBG structure can achieve 270 MHz–20 GHz bandwidth in a reference of −30 dB, which is wide in range. The measured and simulated results indicate the wideband of noise suppression. In addition, the lower and upper cutoff frequencies are estimated by using equivalent circuit models, respectively. Moreover, the IR-Drop and dc resistance is accurately investigated through 3-D simulations. Finally, the transfer characteristics of single signal line are studied.

1. INTRODUCTION

With the rapid development in integrated electronic systems, the clock frequency has reached at GHz level with faster transmission speed of signals, and data up and down time factors have been much steeper for the modern integrated circuits. The increase in high-speed clock frequency introduces serious power integrity (PI) problems and ground bounce noise (GBN), especially the inevitable Simultaneous Switching Noise (SSN) caused by the continuous switching off of a large number of drive switches. SSN can result in a degradation of the signal integrity (SI) and a significant decline in system stability [1–3].

Many noise suppression methods have been developed to mitigate the effect of SSN including using decoupling capacitors, selecting the number and location of the vias and using differential interconnects [4]. However, these methods have some disadvantages that either they cannot provide efficient suppression of noise at high frequency or they are expensive to implement. Hence, a new-type structure called electromagnetic band gap (EBG) structure is brought forward to suppress this kind of noise.

The EBG structure was originally derived from photonic band gap (PBG) structure in optics [5]. Since the EBG structure has the characteristic of prohibiting the propagation of electromagnetic waves within a certain bandwidth, it has wide advantages for SSN suppression such as wider bandwidth and deeper suppression depth. EBG structure has been widely developed in the filter [6, 7] and the antenna [8, 9].

In recent years, several types of EBG structures have been developed to inhibit SSN. Three-dimensional (3-D) embedding structures represented by mushroom-type EBG structure [10–14] can suppress SSN, but the production cost is too high. Coplanar compact EBG structures represented by L-bridge EBG structure [15–17] and other bridge EBG structures are presented, but the bandwidth of suppression is limited.

Received 16 February 2017, Accepted 22 April 2017, Scheduled 2 May 2017

* Corresponding author: Xiu-Jie Hu (18729571536@163.com).

[1] Key Lab of High-Speed Circuit Design and EMC, Ministry of Education, Xidian University, Xi'an, Shaanxi 710071, China. [2] Institute of Electronic CAD, Xidian University, Xi'an, Shaanxi 710071, China.

A novel Z-EBG structure embedded by a double complementary slit ring resonator (DBCSRR) is proposed in this paper. Based on the previous work, the DBCSRR is embedded in the Z-bridge structure to obtain better suppression of SSN. A wide stopband for the suppression against SSN propagation extenging from 270 MHz to 20 GHz at −30 dB is achieved. At the end of the paper, the time-domain eye diagram is used to verify the application of this structure to meet the signal integrity requirements of high-speed circuits.

2. STRUCTURE DESIGN

The new structure is based on the existing Z-bridge EBG structure, by adding DBCSRR structure in some of the cells to improve the SSN suppression capability of the structure. As shown in Fig. 1. The power plane is a graphical EBG plane. It consists of five Z-bridge structural elements embedded with DBCSRR structures and four Z-bridge structural elements. The topography is shown in Fig. 1(a) and the side view shown in Fig. 1(b).

The structure of Z-bridge EBG unit with embedded DBCSRR structure is shown in Fig. 2. The corresponding parameters are $a_1 = 30\,\text{mm}$, $a_2 = 27.4\,\text{mm}$, $a_3 = 22.4\,\text{mm}$, $b_1 = 28.8\,\text{mm}$, $g_1 = 0.5\,\text{mm}$, $g_2 = 0.5\,\text{mm}$, $g_3 = 0.2\,\text{mm}$, $g_4 = 0.2\,\text{mm}$, $g_5 = 1.7\,\text{mm}$, $w_1 = 0.2\,\text{mm}$, $w_2 = 0.4\,\text{mm}$, $w_3 = 0.1\,\text{mm}$, $w_4 = 0.4\,\text{mm}$, $w_5 = 0.4\,\text{mm}$. The substrate material is FR-4 with a relative permittivity 4.4 and loss

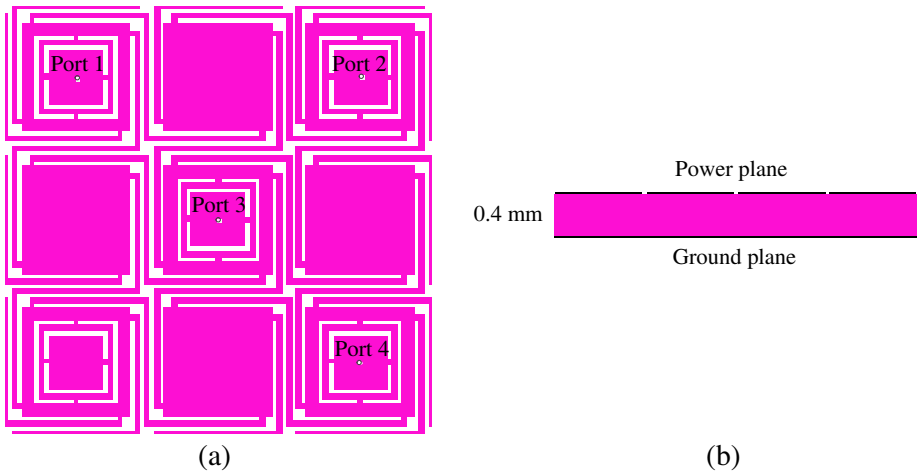

Figure 1. The presented novel EBG structure: (a) Top view. (b) Side view.

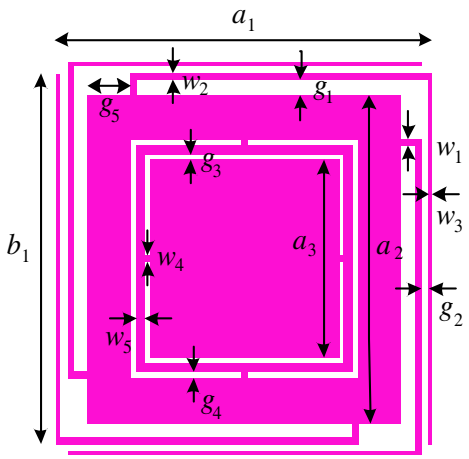

Figure 2. Unit of Z-bridge EBG embedded DBCSRR structure.

tangent of 0.02. The thickness of the substrate is 0.4 mm and the thickness of the copper foil is 0.035 mm. To verify the performance of this architecture for SSN noise suppression, four 50 Ω lumped coaxial ports were set up, with Port 1 as the input port and Port 2–Port 4 as the output ports. Each port location is in the center of each cell.

In order to obtain the power supply noise suppression capability of the proposed structure, the structure is simulated by Ansoft HFSS V15, and the amplitude of the S parameter between the required ports is obtained finally. Fig. 3 shows the simulated and measured S-parameters for the designed novel EBG structure. As shown in Fig. 3, the proposed EBG structure has a good behavior that its SSN suppression (S_{21}) is observed starting at approximately 270 MHz and extending to 20 GHz at −30 dB suppression of the band gap depth. It can be seen that the Z-bridge EBG with embedded DBCSRR structure has a good noise suppression effect at −30 dB suppression depth, and the suppression effect is superior to the L-bridge EBG structure and Z-bridge EBG structure. Simultaneously, the simulated result is similar to the measured one as shown in Fig. 3(b) by the vector network analyzer (VNA).

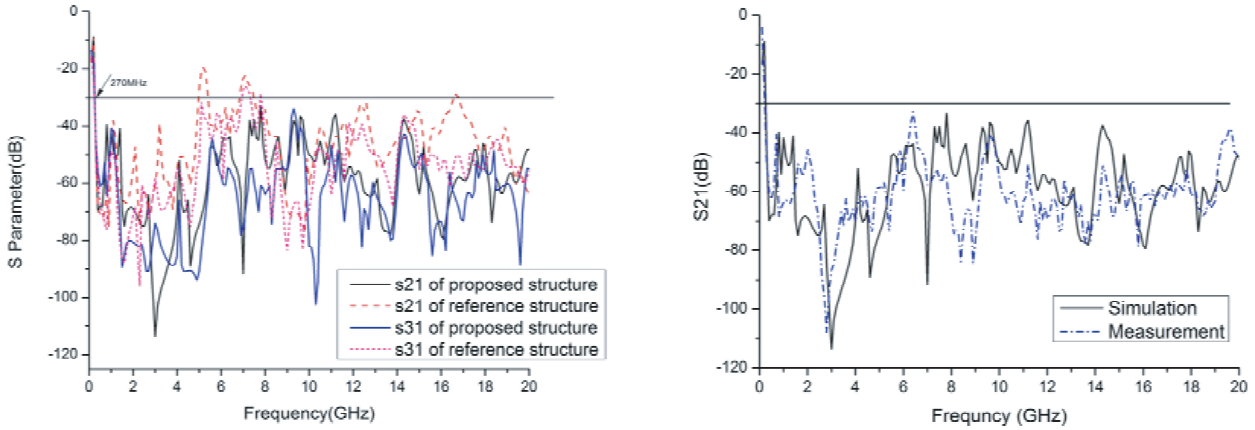

Figure 3. Simulated and measured S-parameter for the designed novel EBG structure. (a) The simulated S-parameter for the designed novel EBG structure. (b) Comparison of the simulation and measurement of S_{21} for proposed structure.

3. THEORETICAL ANALYSIS FOR PROPOSED STRUCTURE

3.1. The Estimate of the Lower Cutoff Frequency f_L

The EBG structure is functionally equivalent to a low-pass filter composed of a plurality of lumped circuit elements, when works in the low hundreds of MHz. These elements are determined by the overall size of the EBG cell. The lumped parameters of these components include the parallel-plate capacitance C_p, wide conductor loop inductance L_p, bridge microstrip capacitance C_b, bridge partial inductance L_b and gap coupling capacitance between the neighboring metal patches C_g. The formulas can be derived as [18–20], respectively:

$$C_p = \varepsilon_0 \varepsilon_r \frac{S}{h} \tag{1a}$$

$$L_p = \mu_0 h \frac{len}{W} \tag{1b}$$

$$C_b = len \cdot \frac{0.67(1.41 + \varepsilon_r)}{\ln\left(\frac{7.5h}{W}\right)} \tag{1c}$$

$$L_b = len \cdot k \cdot \ln\left(2\pi \frac{h}{W}\right) \tag{1d}$$

$$C_g = \frac{\varepsilon_0(1+\varepsilon_r)l}{\pi}\cos h^{-1}\left(\frac{p}{g}\right) \tag{1e}$$

where ε_0 and μ_0 are the permittivity and permeability of free space respectively. ε_r is the relative dielectric constant, S the projective area, h the substrate thickness between the power plane and ground plane, *len* the length of the microstrip line, w the width of the line, k a constant 0.2 nH/mm, l the side length of the patch of EBG unit, p the cycle of EBG units, and g the gap between the adjacent units.

The equivalent model consists of three parts. The first part describes the propagation characteristics between the traditional EBG patch and the solid ground plane, represented by the equivalent capacitance $C_{pl} = 73.086\,\text{pF}$ and inductance $L_{pl} = 0.5\,\text{nH}$. The second part characterizes the bridge effect, represented by the bridge inductance $L_{bl} = 42.5718\,\text{nH}$, bridge capacitance C_{bl1} and C_{bl2}, $C_{bl} = 2C_{bl1} + C_{bl2} = 3.52\,\text{pF}$. And in the third part, C_{bp} and L_{bp} are the equivalent capacitance and equivalent inductance of the inner parallel-plate of the DBCSRR. C_{bbn} and L_{bbn} denote the capacitance and parallel inductance of the coplanar waveguide in the DBCSRR resonator.

$$C_{bp} = \varepsilon_0\varepsilon_r\frac{d^2}{h} \tag{1f}$$

$$L_{bp} = \mu_0 h \tag{1g}$$

$$C_{bbn} = 4\varepsilon_0\varepsilon_r w_1(d+2s+w_1)/h \tag{1h}$$

$$L_{bbn} = (d+2s+w_1)L_{pul} \tag{1i}$$

L_{pul} is the inductance of per unit length of the coplanar waveguide.

$$L_{pul} = Z_{\text{CPW}}\sqrt{\varepsilon_{effc}}/c \tag{1j}$$

where Z_{CPW} and ε_{effc} are the impedance and effective permittivity of the coplanar waveguide, and c is the velocity of light in free space and d^2 the projective area of DBCSRR resonator. The joint between the novel structure units can be modeled with the equivalent circuit as shown in Fig. 4(a). The equivalent capacitance and equivalent inductance of the inner parallel-plate of the DBCSRR $C_{bp} = 48.846\,\text{pF}$ and $L_{bl} = 42.5718278\,\text{nH}$, the capacitance and parallel inductance of the coplanar waveguide in the DBCSRR resonator $C_{bbn} = 3.613\,\text{pF}$ and $L_{bbn} = 8.527749\,\text{nH}$.

The bridge capacitance C_{bl} and gap capacitance between the joint C_g can be ignored for that they are extremely large in the frequency range of interest. So the equivalent circuit can be simplified to a single resonance circuit model, as shown in Fig. 4(b).

As a result, the lower cutoff frequency of the new EBG can be derived from resonance frequency of the parallel LC resonator in Eq. (2).

$$f_L = \frac{1}{\pi}\sqrt{\frac{C_{pl}+C_{bp}}{\left(L_{pl}+\dfrac{L_{bbn}}{2}+L_{bl}\right)\cdot C_{pl}\cdot C_{bp}}} \tag{2}$$

Based on Eqs. (1)–(2) and the new EBG structure dimensions, the calculated results are following $f_L = 261.583\,\text{MHz}$. So f_L is approximate to the simulation on f_L.

3.2. Discussion of the Cutoff Frequency f_H

Similarly, the circuit element L_{bl} can be ignored for analyzing the high cutoff frequency according to Fig. 4, and the impedance of the equivalent circuit can be calculated. The Z can be derived as

$$Z = \left(j\omega\frac{L_{bp}}{2}+\frac{2}{j\omega(C_{bp}+C_g)}\right)\Big\|\left(j\omega\frac{L_{bp}}{2}+\frac{2}{j\omega(C_{pl}+C_g)}\right) \tag{3}$$

$$Z = \frac{-\omega^4 L_{pb}^2(C_{bp}+C_g)(C_{pl}+C_g)+4\omega^2(C_{bp}+C_{pl}+2C_g)-16}{4j\left[\omega^3 L_{bp}(C_{bp}+C_g)(C_{pl}+C_g)-2\omega(C_{bp}+C_{pl}+2C_g)\right]} \tag{4}$$

where $Z = \frac{P(\omega)}{Q(\omega)}$ and

$$Q(\omega) = 4j\left[\omega^3 L_{pb}(C_{pb}+C_g)(C_{pl}+C_g)-2\omega(C_{pb}+C_{pl}+2C_g)\right] \tag{5}$$

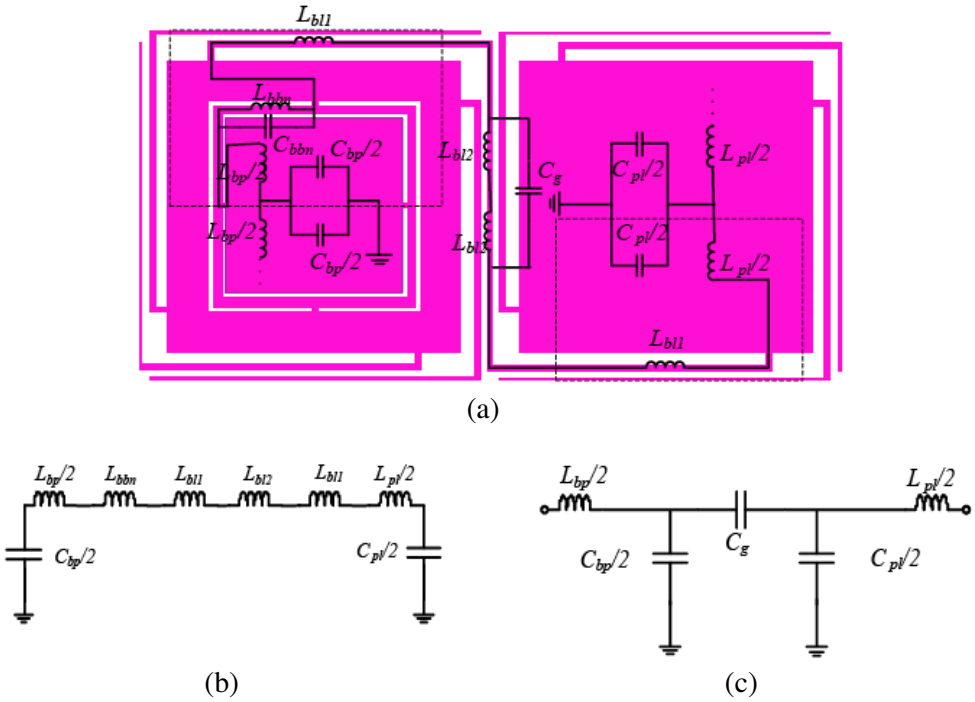

Figure 4. Equivalent circuit for the joint between Z-bridge EBG structure units. (a) Complete model. (b) Lower cutoff frequency simplified model. (c) Higher cutoff frequency simplified model.

If Z tends to infinity and $Q(\omega) = 0$, as

$$\omega^2 L_{pb}(C_{pb} + C_g)(C_{pl} + C_g) - 2(C_{pb} + C_{pl} + 2C_g) = 0 \tag{6}$$

$$\omega = \sqrt{\frac{2(C_{pb} + C_{pl} + 2C_g)}{L_{pb}(C_{pb} + C_g)(C_{pl} + C_g)}} \tag{7}$$

$$f_H = \frac{1}{2\pi}\sqrt{\frac{2(C_{pb} + C_{pl} + 2C_g)}{L_{pb}(C_{pb} + C_g)(C_{pl} + C_g)}} = 18.7\,\text{GHz} \tag{8}$$

3.3. Analysis of IR-Drop

The dc current flow causes a voltage drop (known as IR-drop) across the EBG plane [21]. And the IR-drop of a planar EBG plane needs to be considered when it is used for the power distribution network (PDN). The dc resistance of the proposed structure is larger than that of the integrated power and ground plane because of the Z-bridges [22]. Therefore, the IR-drop of the proposed EBG is evaluated across the patterned plane by using CST EM Studio in this paper.

The proposed EBG simulates the worst example that the distance between the two ports is farthest. It is able to calculate the voltage distribution on the plane by adding two perfect electric conductor (PEC) auxiliary bricks for injecting the 1 A DC current [15]. Figs. 5(a) and (b) show the dc-drop between the current ports on the power plane and the ground plane, respectively. According to the results of the simulation, the overall voltage differences on the power plane and the ground plane are 145.725 mV and 0.545 mV, respectively, which corresponding to the dc resistance are 145.725 mΩ and 0.545 mΩ based on Ohm's Law. Fig. 6 shows that the overall voltage difference on the power plane of the Z-EBG is 133.388 mV. So the dc resistance is 133.388 mΩ. By contrast, the dc resistance increases 12.337 mΩ because of the inserted DBCSRR structure.

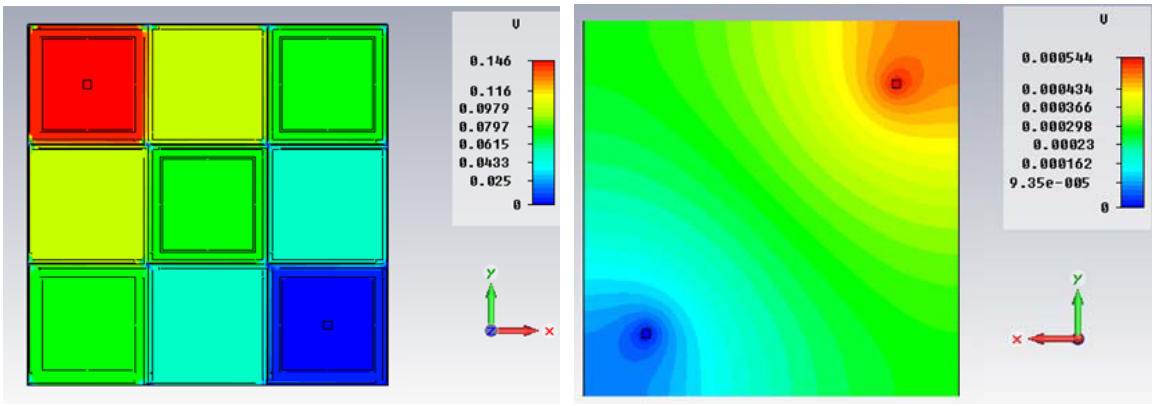

(a) (b)

Figure 5. Voltage distribution for the proposed structure. (a) Power plane. (b) Ground plane.

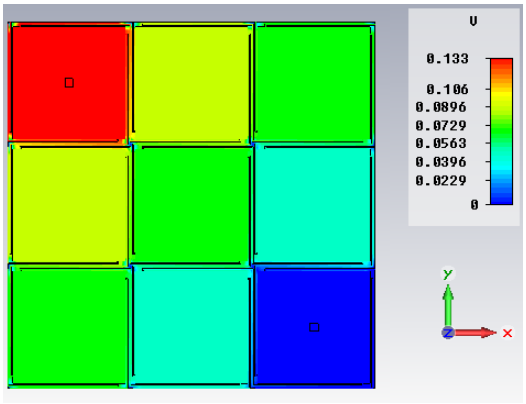

Figure 6. Voltage distribution for the traditional Z-EBG structure.

4. SIGNAL INTEGRITY OF THE PROPOSED STRUCTURE

Although the novel proposed EBG structure can effectively suppress the SSN, it leads to deterioration of signal transmission quality because the power plane is not complete. Therefore, it is necessary to analyze the signal transmission characteristics. As shown in Fig. 7(a), we consider a transmission line with a length of 60 mm. The trace propagates from the first layer to the forth layer and back to the first layer with two via transitions along the path. The second and third layers of the PCB are the patterned power plane and the solid ground plane, respectively. The space between adjacent layers is 0.4 mm. Besides, Port 1 and Port 2 are located at both ends of the signal line. The side view of PCB is shown in Fig. 7(b).

A nonreturn to zero (NRZ), pseudo random binary sequence (PRBs) is sent at Port 1, and the signal propagation characteristics are monitored at Port 2. The transmitted PRBs is coded at 2.5 Gb/s, with 0.5 V swing, and the nominal rise/fall time is 125 ps. The eye patterns of the L-EBG plane and the proposed structure are generated by using Ansoft Designer V4, as shown in Fig. 8. It is seen that

Table 1. Comparison result of the L-EBG and the proposed EBG structure.

	MEO	MEW
L-EBG	225 mv	350 ps
Proposed EBG	250 mv	420 ps

MEO = 225 mV, and MEM = 350 ps for L-EBG, and MEO = 250 mV and MEW = 420 ps for the proposed EBG board respectively, as shown in Table 1.

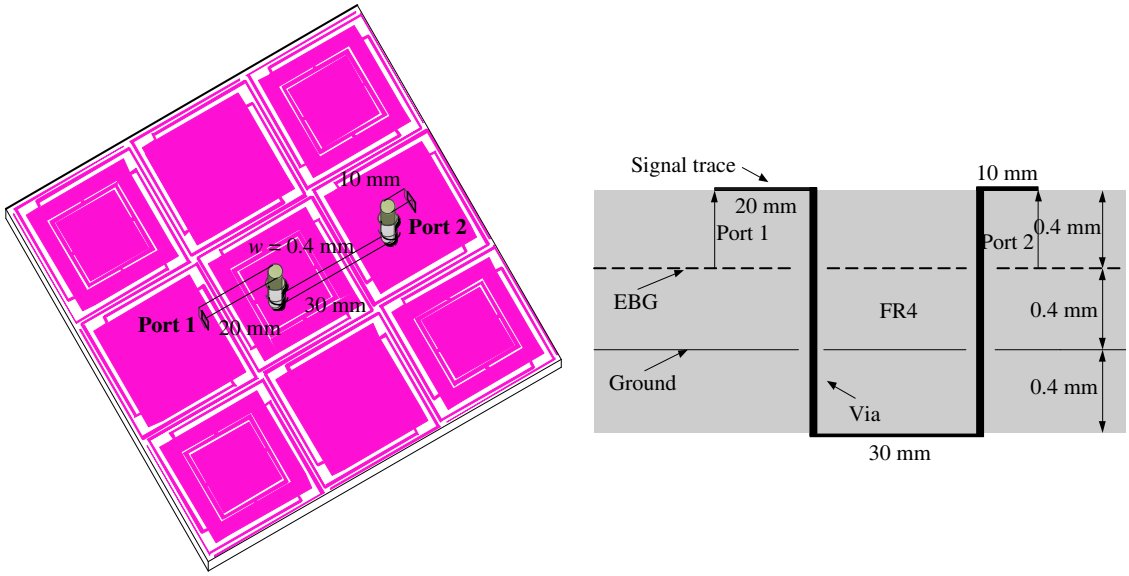

(a) (b)

Figure 7. Four-layer structure with single-ended trace transmit between the patterned power plane and solid ground plane. (a) The three-dimensional view. (b) The side view.

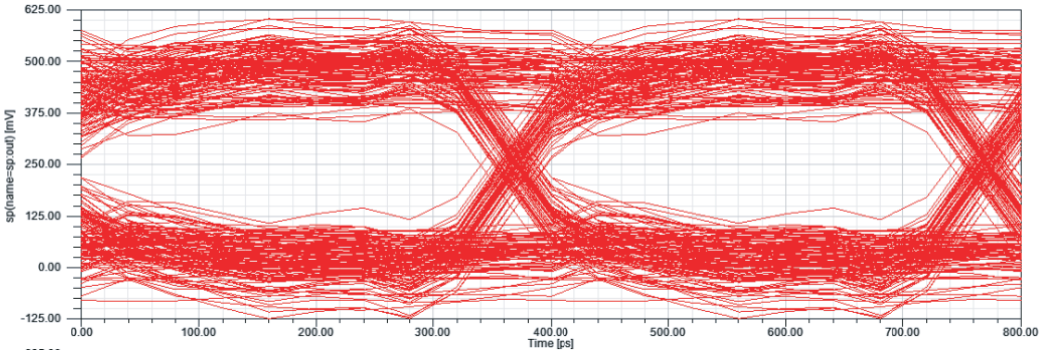

(a)

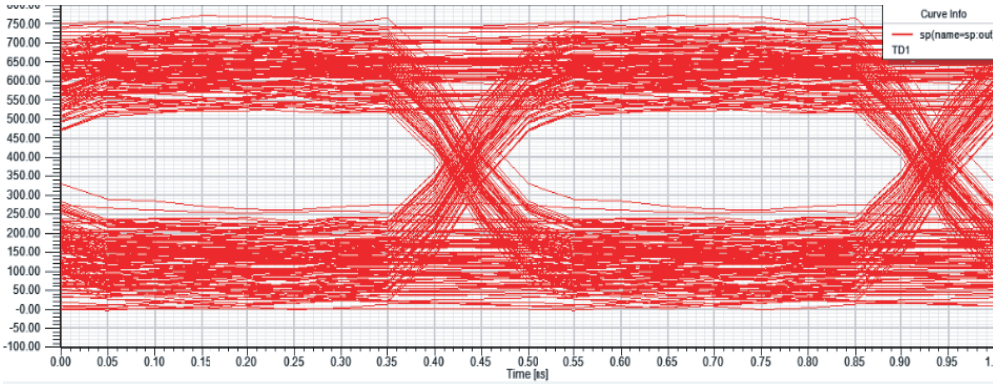

(b)

Figure 8. Simulated eye patterns for (a) the L-EBG board and (b) the proposed EBG board.

5. CONCLUSION

To conclude, a novel Z-EBG structure embedded by a DBCSRR filter is proposed in this paper to enhance the ability of SSN suppression. Compared with the traditional L-bridge EBG structure, the novel structure has a great improvement on the width of stopband and suppression depth. The stopband ranges from 270 MHz to more than 20 GHz at the restraining depth of −30 dB. Meanwhile, we use equivalent circuit models to analyze lower cutoff and upper frequency of the proposed structure, respectively. Then analysis of IR-Drop and DC resistance is obtained by CST simulation. Finally, the effect of the new structure on SI is investigated. And the structure is met with signal integrity by time-domain simulation results in high-speed circuit.

REFERENCES

1. Qin, J. and O. M. Ramahi, "Ultra-wideband mitigation of simultaneous switching noise using novel planar electromagnetic bandgap structures," *IEEE Microwave and Wireless Components Letters*, Vol. 16, No. 9, 1531–1309, 2006.
2. Kwon, J. H., D. U. Sim, S. I. Kwak, and J. G. Yook, "Novel electromagnetic bandgap array structure on power distribution network for suppressing simultaneous switching noise and minimizing effects on high-speed signals," *IEEE Trans. Electromagn. Compat.*, Vol. 52, No. 2, 365–372, 2010.
3. Kim, S.-G., H. Kim, H.-D. Kang, and J.-G. Yook, "Signal integrity enhanced ebg structure with a ground reinforced trace," *IEEE Transactions on Electronics Packing Manufacture*, Vol. 55, No. 2, 373–380, 2010.
4. Zhang, M. S., Y. S. Li, C. Jia, et al., "A power plane with wideband SSN suppression using a multi-via electromagnetic bandgap structure," *IEEE Microwave and Wireless Components Letters*, Vol. 17, No. 4, 307–309, 2007.
5. Zhu, H., J. Li, and J. Mao, "Ultra-sideband suppression of SSN using localized topology with CSRRs and embedded capacitance in high-speed circuits," *IEEE Transactions on Microwave Theory and Techniques*, Vol. 61, No. 2, 764–772, 2013.
6. De Paulis, F., M. Cracraft, C. Olivieri, S. Connor, A. Orlandi, and B. Archambeault, "EBG-based common-mode stripline filters: Experimental investigation on interlayer crosstalk," *IEEE Trans. Electromagn. Compat.*, Vol. PP, No. 99, 19, Jul. 2015.
7. Anand, A., K. Shambavi, and Z. C. Alex, "Design Of UWB band pass filter with inter digitalcoupled lines and circular shaped EBG structure," *International Conference on Green Computing Communication and Electrical Engineering (ICGCCEE)*, 1–4, Mar. 6–8, 2014.
8. Gujral, M., J. L.-W. Li, T. Yuan, and C.-W. Qiu, "Bandwidth improvement of microstrip antenna array using dummy EBG pattern on feedline," *Progress In Electromagnetics Research*, Vol. 127, 79–92, 2012.
9. Kim, S.-H., T. T. Nguyen, and J.-H. Jang, "Reflection characteristics of 1-D EBG ground plane and its application to a planar dipole antenna," *Progress In Electromagnetics Research*, Vol. 120, 51–66, 2011.
10. Wu, T. L., S. T. Chert, J. N. Huang, and Y. H. Lin, "Numerical and experimental investigation of radiation caused by the switching noise on the partitioned dc reference planes of high speed digital PCB," *IEEE Trans. Electromagn. Compat.*, Vol. 46, No. 1, 33–45, Feb. 2004.
11. Wu, T. L., H. H. Chuang, and T. K. Wang, "Overview of power integrity solutions on package and PCB: Decoupling and EBG isolation," *IEEE Trans. Electromagn. Compat.*, Vol. 52, No. 2, 346–356, May 2010.
12. Zhu, H.-R. and J.-F. Mao, "Localized planar EBG structure of CSRR for ultrawideband SSN mitigation and signal integrity improvement in mixed-signal systems," *IEEE Trans. Compon. Packag., Manuf. Technol.*, Vol. 3, No. 12, 2092–2100, Dec. 2013.
13. Yang, F.-R., K.-P. Ma, Y. Qian, and T. Itoh, "A uniplanar compact photonic-bandgap (UC-PBG) structure and its applications for microwave circuits," *IEEE Transactions on Microwave Theory and Techniques*, Vol. 47, No. 8, 1509–1514, Aug. 1999.

14. Li, L., B. Li, H.-H. Liu, and C.-H. Liang, "Locally resonant cavity cell model for electromagnetic bandgap structures," *IEEE Trans. Antennas Propag.*, Vol. 54, No. 1, 90–100, Jan. 2006.
15. Rao, P. H. and M. Swaminathan, "A novel compact electromagnetic bandgap structure in power plane for wideband noise suppression and low radiation," *IEEE Trans. Electromagn. Compat.*, Vol. 53, No. 4, 996–1004, Nov. 2011.
16. Shi, Y., W. Tang, S. Liu, X. Rao, and Y. L. Chow, "Ultra-wideband suppression of power/ground noise in high-speed circuits using a novel electromagnetic bandgap power plane," *IEEE Trans. Compon. Packag., Manuf. Technol.*, Vol. 3, No. 4, 653–660, Apr. 2013.
17. Yuan, H., L. Fang, C. Li, S. Bo, and W. Guan, "Signal integrity analysis of localized new EBG structure for ultra-wideband simultaneous switching noise suppression," *2014 3rd Asia-Pacific Conference on Antennas and Propagation (APCAP)*, 1444–1446, Jul. 26–29, 2014.
18. Bogatin, E., *Signal and Power Integrity — Simplified*, 2nd Edition, Pretince Hall, NJ, 2009.
19. Kim, K. H. and J. E. Schutt-Ainé, "Analysis and modeling of hybrid planar-type electromagnetic-bandgap structures and feasibility study on power distribution network applications," *IEEE Transactions on Microwave Theory and Techniques*, Vol. 56, No. 1, 178–186, Jan. 2008.
20. Kim, K. H. and J. E. Schutt-Ainé, "Design of EBG power distribution networks with VHF-band cutoff frequency and small unit cell size for mixed-signal systems," *IEEE Microwave and Wireless Components Letters*, Vol. 17, No. 7, Jul. 2007.
21. De Paulis, F., L. Raimondo, and A. Orlandi, "IR-drop analysis and thermal assessment of planar electromagnetic bandgap structures for power integrity applications," *IEEE Trans. Adv. Packag.*, Vol. 33, No. 3, 617–622, Aug. 2010.
22. Kim, T. H., D. Chung, E. Engin, W. Yun, Y. Toyota, and M. Swaminathan, "A novel synthesis method for designing electromagnetic bandgap (EBG) structures in packaged mixed signal systems," *Proc. 56th Electron. Compon. Technol. Conf.*, 1645–1651, May 30–Jun. 2, 2006.